Turkish Journal of Electrical Engineering & Computer Sciences

http://journals.tubitak.gov.tr/elektrik/

Research Article

Turk J Elec Eng & Comp Sci
(2017) 25: 4624 – 4635

doi:10.3906/elk-1701-225

# A modified two-degree of freedom-internal model control configuration for load frequency control of a single area power system

**Bheem SONKER, Deepak KUMAR*, Paulson SAMUEL**
Department of Electrical Engineering, Motilal Nehru National Institute of Technology Allahabad, Uttar Pradesh, India

**Received:** 23.01.2017 • **Accepted/Published Online:** 17.08.2017 • **Final Version:** 03.12.2017

**Abstract:** In this paper, we propose a modified two degree-of-freedom internal model control structure, with dual feedback loop configuration for the load frequency control problem of a single-area power system. Our main objective is to achieve better transient and steady state performance. The predictive model of the proposed configuration is derived through the stability equation method, which preserves the stability of the model. The proposed scheme is simulated for a single-area power system with nonreheated turbine and 50% parametric uncertainty. It is observed from the responses and the performance indices that the proposed control configuration gives better results compared to well-known existing techniques.

**Key words:** Two degree-of-freedom internal model control, load frequency control, model order reduction, robustness

## 1. Introduction

In general, the load frequency control (LFC) problem concerns the control of the real power output of generating units, due to changes in the system frequency and the tie-line power interchange within specified limits [1]. The transmission lines that connect the generation, transmission, and distribution systems are called tie lines. During the operation of the power system, the role of LFC is essential if the fluctuations occur in tie-line power interchange [2], due to random changes in load demand and external disturbance. Therefore, the power system should be stable and robust enough for specified voltage levels in order to sustain the external disturbance and parameter uncertainties in case of transient disturbances.

In the last few decades, several approaches have been proposed for LFC, using various control strategies such as classical control [2], suboptimal control [3], adaptive control [4], variable structure control [5,6], self-tuning control [7], artificial neural network [8], fuzzy logic [9,10], robust LFC using a genetic algorithm [11], particle swarm optimization [12–14], tabu search [15,16], and bacteria foraging optimization [17,18]. This study shows the implementation of TDF-IMC for the LFC problem and focuses on TDF-IMC application. Recently, Ghousiya et al. [19] presented an IMC-based proportional-integral-derivative (PID) controller with optimal $H_2$ minimization. Saxena and Hote [20] presented various developments and future aspects of IMC for maintaining robust performance and disturbance rejection. Moreover, in [21], an internal model control-proportional integral derivative (IMC-PID) controller is designed for turbine control loop. Liu and Gao [22] discussed a modified design of the internal model control to improve closed-loop system performance with load

*Correspondence: deepak_kumar@mnnit.ac.in

disturbance rejection. Later, Morsali et al. [23] designed a thyristor-controlled series capacitor-based controller for automatic generation control (AGC) of an interconnected multiarea power system, using fractional order PID (FOPID) approach to obtain robust performance. Zamani et al. [24] implemented the gases Brownian motion optimization (GBMO)-based FOPID controller for load frequency control by considering governor saturation. Furthermore, a PID plus second-order derivative controller, based on lion optimization and teaching–learning optimization-based two-degree freedom PID controller, are proposed in [25] and [26], respectively. The fractional order fuzzy PID controller [27] is designed with a bacterial foraging optimization algorithm for a multiarea, multisource power system. Several other versions of FOPID controller for the LFC problem of single/multiarea power systems can be found in [28–31]. As this article is related to the internal model control (IMC) design for the LFC problem, a detailed survey of LFC is avoided due to space limitation. However, an exhaustive survey of LFC approaches can be found in [32,33]. As far as LFC through IMC scheme is concerned, interested readers may refer to [34–36]. Tan [34,35] used a two-degree-of-freedom IMC (TDF-IMC) scheme to tune the PID controller for LFC of a single-area power system with nonreheated, reheated, and hydro turbines, and presented a robustness analysis by introducing uncertainty into the parameters. Later, Saxena and Hote [36] used model order reduction for employing the IMC for LFC of a single-area case. Recently, Padhan and Majhi [37] tuned a PID controller using Laurent series expansion, and extended the approach to a multiarea case by performing robustness analysis. Subsequently, Anwar and Pan [38] introduced a direct synthesis approach for PID controller design through frequency response matching. Further, a fractional order PID controller [30,32] is designed for a single area power system, which provides robustness towards parameter uncertainties and disturbance rejection.

This paper discusses the development of a modified TDF-IMC configuration, by employing the reduced-order modelling concept [39] for the derivation of a predictive model for IMC configuration. The proposed TDF-IMC structure is a combination of double feedback loops and fulfils the following objectives: (1) it reduces the frequency deviation with minimization of steady state error, settling time, peak overshoot, and oscillations; (2) it provides robustness of system model with parametric uncertainty; (3) it achieves faster load disturbance rejection. The paper is organized as follows. A brief description of a single area power system is included in Section 2, and the proposed approach is discussed in Section 3. Simulation results with nominal and perturbed parameters are given in Section 4. Finally, concluding remarks are presented in Section 5.

## 2. Plant under consideration

A linearized single-area power system [1] is considered for the analysis, as shown in Figure 1. It consists of a governor with dynamics $G_G(s) = 1/(sT_G + 1)$, load and machines with dynamics $G_P(s) = K_P/(sT_P + 1)$, droop characteristics $1/R$, and a nonreheated turbine with dynamics $G_T(s) = 1/(sT_T + 1)$. $1/R$ is a feedback gain to improve the damping properties of the power system. Furthermore, $K_P$ is the electric system gain, $T_P$ is the electric time constant in second, $T_T$ is the nonreheated turbine time constant in second, $T_G$ is the governor time constant in second, $R$ is the speed regulation due to governor in Hz/p.u. MW, $\Delta P_d$ is the load disturbance in p.u. MW, and $\Delta f$ is the change in frequency. $G(s)$ and $G_d(s)$ are transfer functions with respect to reference input and load disturbance, respectively.

Hence, the overall system model is

$$\Delta f\,(s) = G\,(s)\,u\,(s) + G_d\,(s)\,\Delta P_d\,(s)\,, \tag{1}$$

where $G\,(s) = \frac{G_P(s)G_G(s)G_T(s)}{1+G_P(s)G_G(s)G_T(s)\frac{1}{R}}$ and $G_d\,(s) = \frac{G_P(s)}{1+G_P(s)G_G(s)G_T(s)\frac{1}{R}}$.

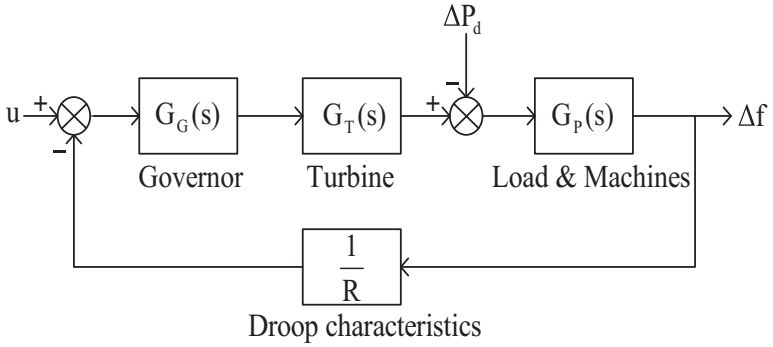


**Figure 1.** Linearized single-area power system model.

It is clear that LFC is a load disturbance rejection problem that uses feedback $u(s) = -G_c(s)\Delta f(s)$ to stabilize the plant $G(s)$ under load disturbance $\Delta P_d(s)$, and reduces the effect of $\Delta P_d(s)$.

## 3. Proposed control configuration

The proposed control configuration contains dual feedback loops for LFC of single-area power system as shown in Figure 2a which is an extension of the TDF-IMC approach [34-36]. The proposed control scheme consists of a linearized single-area power system $G(s)$, $G_m(s)$ as predictive model of $G(s)$, series controller $Q(s)$, TDF-IMC controller $Q_d(s)$, and feedback controller $G_C(s)$. The proposed structure consists of TDF-IMC controller $Q_d(s)$, in the inner loop, whereas feedback controller $G_C(s)$ in the outer loop. A simplified structure of Figure 2a is drawn in Figure 2b, where $K(s) = \frac{Q(s)Q_d(s)}{1+G_m(s)Q(s)Q_d(s)}$ and $G_C(s) = \frac{Q(s)Q_d(s)}{1-G_m(s)Q(s)Q_d(s)}$ are based on the TDF-IMC feedback configuration [35]. The values of tuning parameters $\mu$ and $\mu_d$ of the inner loop are different, whereas they are same in the outer loop for robustness and minimization of the oscillations in the system response. Furthermore, tuning parameters can be assumed to have the same values for both cases, according to parametric uncertainties present in the system. It should be noted that [35] and [36] do not involve dual feedback loop configuration. The design procedure for the proposed TDF-IMC configuration is as follows:

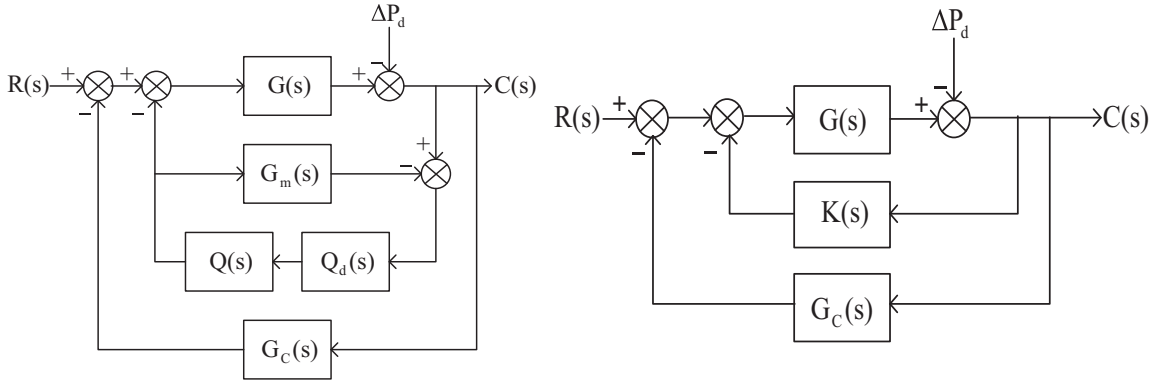


**Figure 2.** a) Proposed control structure; b) simplified proposed control structure.

Consider the transfer function of single-area power system $G(s)$ as

$$G(s) = \frac{G_N(s)}{G_D(s)} = \frac{a_{21}}{a_{11} + a_{12}s + a_{13}s^2 + a_{14}s^3} \tag{2}$$

Initially, predictive model $G_m(s)$ is obtained using the stability equation method [39]. Hence, denominator $G_D(s)$ is factorized into even and odd parts, as given in Eqs. (3) and (4), respectively.

$$G_{De}(s) = a_{11} + a_{13}s^2 = a_{11}(1 + \frac{s^2}{A_1^2}); \text{ where } A_1^2 = \frac{a_{11}}{a_{13}} \tag{3}$$

and

$$G_{Do}(s) = a_{12}s + a_{14}s^3 = a_{12}s(1 + \frac{s^2}{B_1^2}); \text{ where } B_1^2 = \frac{a_{12}}{a_{14}} \tag{4}$$

Now $B_1^2$ is discarded by approximating the stability equation in Eq. (4), as $A_1^2 < B_1^2$, and the denominator of the second-order predictive model is obtained as

$$G_{Dk}(s) = a_{11}(1 + \frac{s^2}{A_1^2}) + a_{12}s = a_{11}^{'} + a_{12}^{'}s + a_{13}^{'}s^2 \tag{5}$$

For the calculation of the numerator of the second-order predictive model, the following table is formed:

$$\begin{array}{lllllll} h_1 = a_{11}a_{21}^{-1} \langle & a_{11} & a_{12} & a_{13} & a_{14} & . & . & . \\ h_2 = a_{21}a_{31}^{-1} \langle & a_{21} & 0 & 0 & 0 & & & \\ & a_{31} & 0 & 0 & 0 & & & \end{array} , \tag{6}$$

where $a_{31} = a_{12} - h_1 a_{22}^{'}$

From Eq. (6), and using Eq. (5) in the first row of the table, the numerator polynomial is obtained and the final predictive model is

$$G_m(s) = \frac{a_{21}' + a_{22}'}{a_{11}' + a_{12}'s + a_{13}'s^2}, \tag{7}$$

where

$$\begin{array}{l} a_{21}^{'} = h_1^{-1}a_{11}^{'} \\ a_{31}^{'} = h_2^{-1}a_{21}^{'} \\ a_{22}^{'} = h_1^{-1}(a_{12}^{'} - a_{31}^{'}) \end{array} \tag{8}$$

Then, $G_m(s)$ is factorized as

$$G_m(s) = G_{m-}(s)\, G_{m+}(s) \tag{9}$$

where $G_{m-}(s)$ is minimum phase and $G_{m+}(s)$ all-pass parts. The series controller is designed by using the low pass filter $f(s)$ as follows:

$$Q(s) = G_{m-}^{-1}(s)\, f(s) \tag{10}$$

with $f(s) = (1 + \mu s)^{-n}$, where $n$ is equivalent to the order of minimum phase. The speed of response of the closed loop system is tuned by $\mu$, which is accountable for the robustness of the system.

Now the TDF-IMC controller [35,36], as second-order low pass filter, is obtained as follows:

$$Q_d(s) = \frac{(\alpha_2 s^2 + \alpha_1 s + 1)}{(\mu_d s + 1)^n}, \tag{11}$$

where $\mu_d$ is tuning parameter and $n$ is an integer to obtain proper/semiproper Q(s). The design of feedback controller $G_c(s)$ is based on the TDF-IMC configuration and the complementary sensitivity function of the TDF-IMC feedback configuration [35], which can be represented by Eqs. (12) and (13), respectively.

$$T(s) = \frac{G_m(s)G_C(s)}{1 + G_m(s)G_C(s)} \tag{12}$$

$$T(s) = G_m(s)Q_d(s)Q(s) \tag{13}$$

We substituted $Q(s)$ and $Q_d(s)$ in Eq. (13), and after further simplification, it resulted in

$$T(s) = \frac{G_m(s)G_m^{-1}(s)\left(\alpha_2 s^2 + \alpha_1 s + 1\right)}{(\mu s + 1)^n \left(\mu_d s + 1\right)^n} \tag{14}$$

By putting $G_m(s) = G_{m+}(s)G_{m-}(s)$ and $\mu = \mu_d$ in Eq. (14), we obtain Eq. (15), as shown below:

$$T\left(s\right) = \frac{G_{m+}(s)\left(\alpha_2 s^2 + \alpha_1 s + 1\right)}{\left(\mu_d s + 1\right)^{2n}} \tag{15}$$

Further, $\alpha_1$ and $\alpha_2$ [35,36], should satisfy

$$\lim_{s \to -p_i} \{1 - T(s)\} = 0, \qquad i = 1, 2 \tag{16}$$

For each pole, $p_1$ and $p_2$ of the second-order predictive model $G_m(s)$. Hence, the values of $\alpha_1$ and $\alpha_2$ are obtained by using Eqs. (15) and (16), as follows:

$$\alpha_2 = \frac{p_1\left(p_1\mu_d - 1\right)^4 - p_2\left(p_1\mu_d - 1\right)^4 - p_1 + p_2}{p_1 p_2\left(p_2 - p_1\right)} \tag{17}$$

$$\alpha_1 = \frac{p_1^2\left(p_2\mu_d - 1\right)^4 - p_2^2\left(p_1\mu_d - 1\right)^4 - p_1^2 + p_2^2}{p_1 p_2\left(p_2 - p_1\right)} \tag{18}$$

By comparing Eqs. (12) and (15), we obtain the following:

$$\frac{G_m(s)G_C(s)}{1 + G_m(s)G_C(s)} = \frac{G_{m+}(s)\left(\alpha_2 s^2 + \alpha_1 s + 1\right)}{\left(\mu_d s + 1\right)^{2n}} \tag{19}$$

After simplifying Eq. (19), $G_C^{nm}(s)$ is obtained as

$$G_C^{nm}(s) = \frac{G_{M-}^{-1}\left(\alpha_2 s^2 + \alpha_1 s + 1\right)}{\{(\mu_d s + 1)^{2n} - G_{M+}(s)\left(\alpha_2 s^2 + \alpha_1 s + 1\right)\}} \tag{20}$$

Then $G_C^{nm}(s)$ is factorized into minimum and all pass parts as follows:

$$G_C^{nm}(s) = G_{C+}^{nm}(s)G_{C-}^{nm}(s), \tag{21}$$

where $G_{C-}^{nm}(s)$ and $G_{C+}^{nm}(s)$ are minimum phase and all-pass part, respectively. Therefore, the final feedback controller is $G_C(s) = G_{C-}^{nm}(s)$.

## 4. Simulation results

Consider the single-area power system [34–36] with a nonreheated turbine as

$$G(s) = \frac{250}{s^3 + 15.88s^2 + 42.46s + 106.2}, \tag{22}$$

where $K_p = 120,\ T_P = 20,\ T_T = 0.3,\ T_G = 0.08,\ R = 2.4.$

Firstly, the predictive model $G_m(s)$ is obtained as

$$G_m(s) = \frac{15.75}{s^2 + 2.674s + 6.687} \tag{23}$$

To check the closeness of the predictive model with $G(s)$, the step responses of $G(s)$, the proposed predictive model $G_m(s)$, and the predictive model used in [36] are drawn in Figure 3. It is clear that the proposed predictive model approximates the single-area power system $G(s)$ well. As explained in the previous section, predictive model $G_m(s)$ is used for computing $Q(s), Q_d(s)$, and, finally, $G_C(s)$.

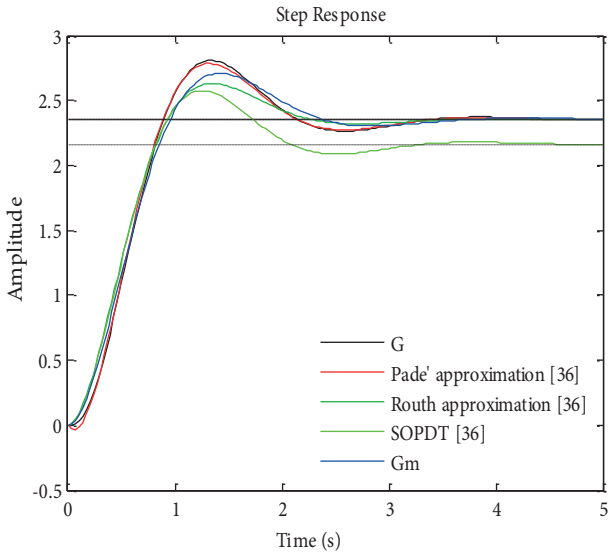


**Figure 3.** Step response of the third-order single-area power system and predictive model.

Taking $\mu = 0.01$ and $n = 2$, the IMC controller $Q(s)$ is obtained as

$$Q(s) = \frac{(s^2 + 2.674s + 6.687)}{15.75(0.01s + 1)^2} \tag{24}$$

and with $\mu_d = 0.1$, the second-order low pass filter $Q_d(s)$ is computed as

$$Q_d(s) = \frac{(0.0707s^2 + 0.3715s + 1)}{(0.1s + 1)^2}, \tag{25}$$

where $\alpha_2 = 0.0707,\ \alpha_1 = 0.3715.$

Now $G_C^{nm}(s)$ is obtained as

$$G_C^{nm}(s) = \frac{0.0707s^4 + 0.5606s^3 + 2.466s^2 + 5.158s + 6.687}{0.001575s^4 + 0.063s^3 - 0.1692s^2 + 0.4495s} \tag{26}$$

Finally, feedback controller $G_C(s)$, as minimum phase of $G_C^{nm}(s)$, is obtained as

$$G_C(s) = \frac{0.0707s^4 + 0.5606s^3 + 2.466s^2 + 5.158s + 6.687}{0.001575s^4 + 0.063s^3 + 0.1692s^2 + 0.4495s} \tag{27}$$

In the present scenario of power system operations, parametric uncertainty is a serious issue that must be addressed with a robust LFC scheme. The robustness of the proposed control configuration is investigated by introducing $\pm 50\%$ parametric uncertainties. Hence, for the nonreheated turbine case, the parameters of the single area power system with uncertainties can be written as

$$\frac{K_P}{T_P} \in [4, 12], \frac{1}{T_P} \in [0.033, 0.1],$$

$$\frac{1}{T_T} \in [2.564, 4.762], \frac{1}{T_G} \in [9.615, 17.857], \tag{28}$$

$$\frac{1}{RT_G} \in [3.081, 10.639]$$

With the implementation of the proposed configuration, simulation results are obtained both with nominal parameters and with 50% parametric uncertainty. To show the effectiveness and performance of the proposed scheme, the external load disturbance $\Delta P_d(t) = -0.01$ at $t = 2$ sec is applied to the system, and results are obtained with the proposed control configuration. The role of the inner and outer loops of the proposed method for nominal value, lower bound, and upper bound are shown in Figures 4a–c, respectively. The following conclusions are drawn from the simulation results:

1. The introduction of the inner loop in the proposed scheme reduces the overall gain of the closed-loop system. However, steady state error is not eliminated to zero value.
2. The outer-loop controller reduces the ill effect of external load disturbance in the system.
3. The inner-loop controller of the proposed scheme controls the undesirable response of the system caused by parametric uncertainties present in the system, which is not controlled by the outer-loop feedback controller.
4. The combination of inner and outer loops of the proposed method reduces settling time, peak overshoot, oscillation, as well as steady state error in the closed-loop response of the system.
5. Disturbance rejection is faster and smoother than in the existing techniques [30,34,36–38].

The result achieved with the nominal parameters is plotted in Figure 5a, and it is clear that it gives better performance than the existing techniques in [30,34,36–38]. Furthermore, Figures 5b and 5c show the responses with lower and upper bound of uncertainty, respectively. Moreover, performance indices, such as integral square error (ISE), integral absolute error (IAE), and integral time absolute error (ITAE), are calculated for the system with nominal parameter and 50% parametric uncertainty. The expressions of ISE, IAE, and ITAE are given as

$$ISE = \int_0^\infty |e(t)|^2 \, dt \tag{29}$$

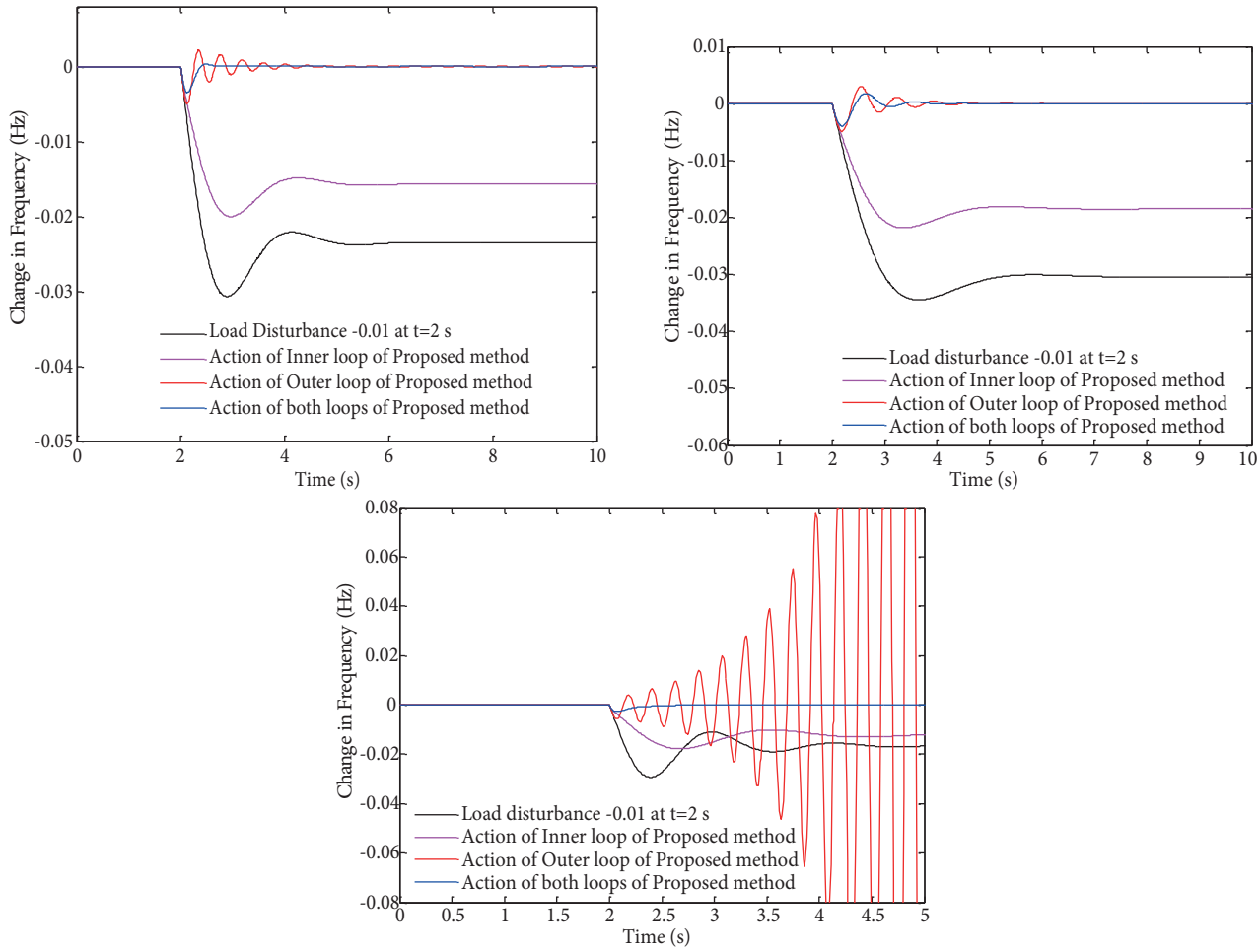


**Figure 4.** a) Action of inner loop, outer loop, and both for nominal value; b) action of inner loop, outer loop, and both for lower bound; c) action of inner loop, outer loop, and both for upper bound.

$$IAE = \int_0^\infty |e(t)|dt \tag{30}$$

$$ITAE = \int_0^\infty t\,|e(t)|\,dt \tag{31}$$

It can readily be seen from Tables 1–3 that the error indices are lower than in the existing techniques [30,34,36–38] in all cases. Therefore, it is concluded that the proposed TDF-IMC configuration handles the frequency deviation more effectively and rejects the disturbance successfully in each case during the power system operation, even with parametric uncertainties.

## 5. Conclusion

The present article developed a new approach for the LFC of a single-area power system as an extension of the TDF-IMC scheme. The inner and outer loop controllers were computed with the help of a predictive model,

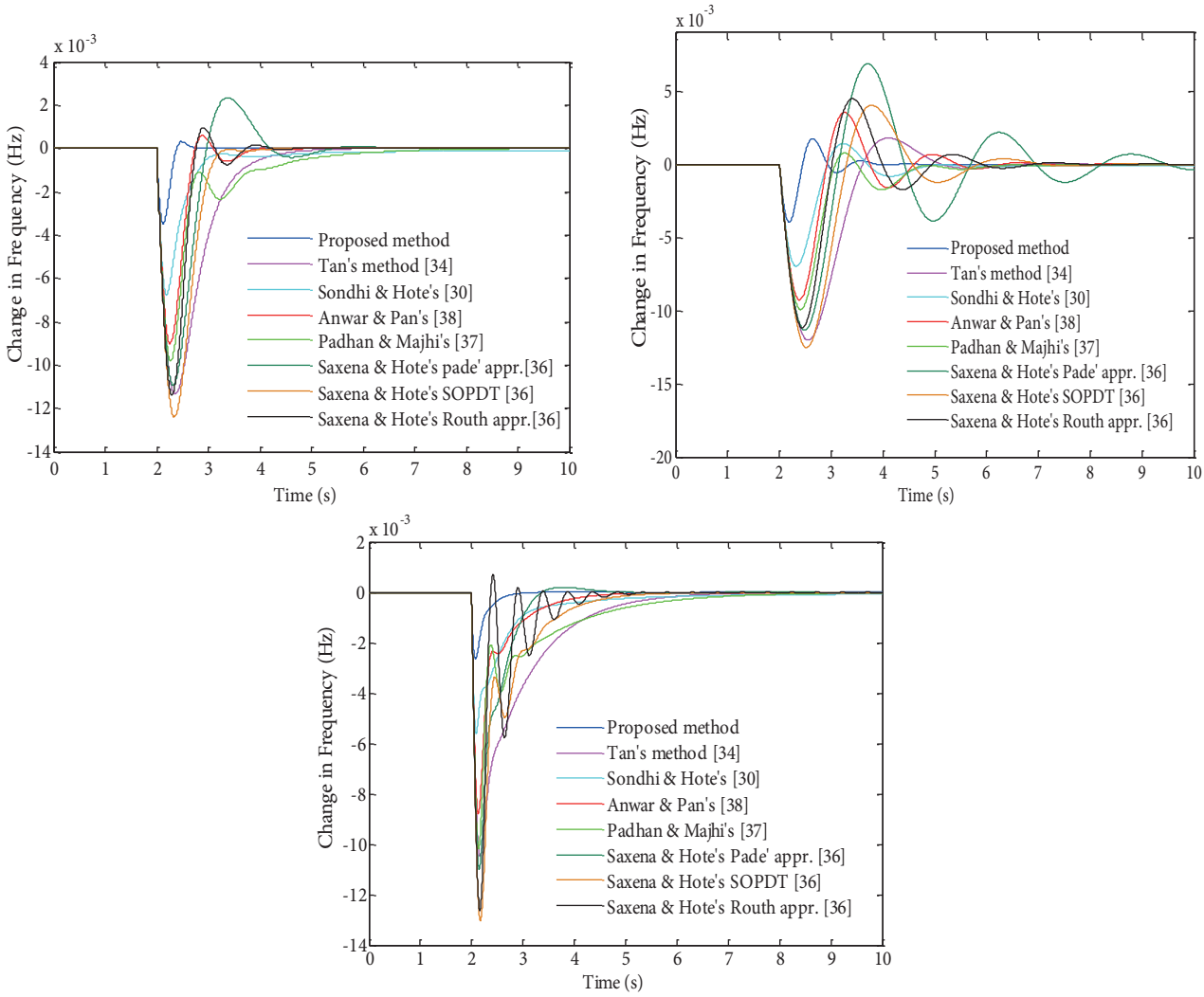


**Figure 5.** a) Responses of proposed and existing methods for nominal value; b) responses of proposed and existing methods with lower bound; c) responses of proposed and existing methods with upper bound.

**Table 1.** Comparison of performance indices for nominal values of parameters.

| Methods | Nominal value | | |
|---|---|---|---|
| | ISE | IAE | ITAE |
| Proposed method | $2.052 \times 10^{-6}$ | 0.0008747 | 0.006768 |
| Sondhi and Hote [30] | $1.364 \times 10^{-5}$ | 0.003877 | 0.0121 |
| Anwar and Pan [38] | $2.615 \times 10^{-5}$ | 0.004261 | 0.03225 |
| Padhan and Majhi [37] | $3.611 \times 10^{-5}$ | 0.007654 | 0.05654 |
| Tan [34] | $7.815 \times 10^{-5}$ | 0.009818 | 0.07114 |
| Sexana and Hote's Padé appr. [36] | 0.0008499 | 0.08183 | 0.4840 |
| Sexana and Hote's SOPDT [36] | 0.0008703 | 0.08166 | 0.4832 |
| Sexana and Hote's Routh appr. [36] | 0.0008231 | 0.08061 | 0.4808 |

which unifies the stability equation method of reduced-order modeling and TDF-IMC. Additionally, results with 50% uncertainty were obtained to check the robustness of the proposed approach with perturbations. It was

**Table 2.** Comparison of performance indices for lower bound of parameters.

| Methods | Lower bound | | |
|---|---|---|---|
| | ISE | IAE | ITAE |
| Proposed method | $4.211 \times 10^{-6}$ | 0.001894 | 0.01419 |
| Sondhi and Hote [30] | $2.221 \times 10^{-5}$ | 0.005813 | 0.01804 |
| Anwar and Pan [38] | $4.42 \times 10^{-5}$ | 0.008581 | 0.05989 |
| Padhan and Majhi [37] | $4.888 \times 10^{-5}$ | 0.008087 | 0.05725 |
| Tan [34] | 0.0001051 | 0.01312 | 0.09257 |
| Sexana and Hote's Padé appr. [36] | 0.0009027 | 0.08336 | 0.4871 |
| Sexana and Hote's SOPDT [36] | 0.0009178 | 0.08329 | 0.4871 |
| Sexana and Hote's Routh appr. [36] | 0.0008657 | 0.08247 | 0.4857 |

**Table 3.** Comparison of performance indices for upper bound of parameters.

| Methods | Upper bound | | |
|---|---|---|---|
| | ISE | IAE | ITAE |
| Proposed method | $1.071 \times 10^{-6}$ | 0.0007117 | 0.005487 |
| Sondhi and Hote [30] | $8.981 \times 10^{-6}$ | 0.003828 | 0.05212 |
| Anwar and Pan [38] | $1.635 \times 10^{-5}$ | 0.004 | 0.02965 |
| Padhan and Majhi [37] | $2.702 \times 10^{-5}$ | 0.007637 | 0.05105 |
| Tan [34] | $5.054 \times 10^{-5}$ | 0.009816 | 0.06888 |
| Sexana and Hote's Padé appr. [36] | 0.0008468 | 0.07998 | 0.4794 |
| Sexana and Hote's SOPDT [36] | 0.0008959 | 0.08118 | 0.4815 |
| Sexana and Hote's Routh appr. [36] | 0.0008091 | 0.07825 | 0.4738 |

observed from the responses and performance indices that the proposed configuration generates better results with the nominal and perturbed parameters. Furthermore, it was observed that the proposed scheme gives better transient and steady state performances with the external load disturbance. In conclusion, the proposed method can be extended to multiarea power systems as well as process control applications.

## References

[1] Kundur P. Power System Stability and Control. New York, NY, USA: McGraw-Hill, 2012.

[2] Concordia C, Kirchmayer LK. Tie-line power and frequency control of electric power systems. T Am Inst Elec Eng 1953; 72: 562-572.

[3] Feliachi A. Load frequency control using reduced order models and local observers. Int J Elec Ener Sys 1987; 7: 72-75.

[4] Liaw CM. Design of a reduced-order adaptive LFC for an interconnected hydrothermal power system. Int J Cont 1994; 60: 1051-1063.

[5] Malik OP, Kumar A, Hope GS. A load frequency control algorithm based on a generalized approach. IEEE T Power Syst 1988; 3: 375-382.

[6] Yang TC, Cimen H, Zhu QM. Decentralized load-frequency controller design based on structured singular values. IEE Proc-C 1998; 145: 7-14.

[7] Lee KA, Yee H, Teo CY. Self-tuning algorithm for automatic generation control in an interconnected power system. Electr Pow Syst Res 1991; 20: 157-165.

[8] Demiroren A, Sengor NS, Zeynelgil HL. Automatic generation control by using ANN technique. Electr Pow Compo Sys 2001; 29: 883-896.

[9] Juang CF, Lu CF. Power system load frequency control by genetic fuzzy gain scheduling controller. J Chin Inst Eng 2005; 28: 1013-1018.

[10] Sinha SK, Patel RN, Prashad R. Application of GA and PSO tuned fuzzy controller for AGC of three area thermal–thermal-hydro power system. Int J Comp Theory Eng 2010; 2: 1793-8201.

[11] Rerkpreedapong D, Hasanovic A, Feliachi A. Robust load frequency control using genetic algorithms and linear matrix inequalities. IEEE T Pow Sys 2003; 18: 855-861.

[12] Juang CF, Lu CF. Load-frequency control by hybrid evolutionary fuzzy PI controller. IEE Proc-C 2006; 153: 196-204.

[13] Hosseini SH, Etemadi AH. Adaptive neuro-fuzzy inference system based automatic generation control. Electr Pow Syst Res 2008; 78: 1230-1239.

[14] Bhatt P, Roy R, Ghoshal SP. Optimized multi area AGC simulation in restructured power systems. Electr Pow Energ Syst 2010; 32: 311-322.

[15] Denna M, Mauri G, Zanaboni AM. Learning fuzzy rules with tabu search-an application to control. IEEE T Fuzzy Sys 1999; 7: 295-318.

[16] Pothiya S, Ngmroo I, Runggeratigul S, Tantaswadi P. Design of optimal fuzzy logic based PI controller using multiple tabu search algorithm for load frequency control. Int J Cont Auto Sys 2006; 4: 155-164.

[17] Chidambaram IA, Paramasivam B. Control performance standards based load-frequency controller considering redox flow batteries coordinate with interline power flow controller. J Power Sources 2012; 219: 292-304.

[18] Debbarma S, Saikia LC, Sinha N. AGC of a multi-area thermal system under deregulated environment using non-integer controller. Electr Pow Syst Res 2013; 95: 175-183.

[19] Ghousiya BK, Seshagiri RA, Radhakrishnan TK. Enhanced IMC based PID controller design for non-minimum phase (NMP) integrating processes with time delays. ISA T 2017; 68: 223-234.

[20] Saxena S, Hote YV. Advances in internal model control technique: a review and future prospects. IETE Tech Rev 2012; 29: 461-472.

[21] Li XF, Chen G, Wang YG. IMC-PID controller design for power control loop based on closed-loop identification in the frequency domain. IFAC-PapersOnLine 2016; 49: 79-84.

[22] Liu T, Gao F. New insight into internal model control filter design for load disturbance rejection. IET Control Theory A 2010; 4: 448-460.

[23] Morsali J, Zare K, Hagh MT. Applying fractional order PID to design TCSC-based damping controller in coordination with automatic generation control of interconnected multi-source power system. ESTIJ 2017; 20: 1-17.

[24] Zamani A, Barakati SM, Darmian SY. Design of a fractional order PID controller using GBMO algorithm for load–frequency control with governor saturation consideration. ISA T 2016; 64: 56-66.

[25] Raju M, Saikia LC, Sinha N. Automatic generation control of a multi-area system using ant lion optimizer algorithm based PID plus second order derivative controller. Electr Pow Energ Syst 2016; 80: 52-63.

[26] Sahu RK, Panda S, Rout UK, Sahoo DK. Teaching learning based optimization algorithm for automatic generation control of power system using 2-DOF PID controller. Electr Pow Energ Syst 2016; 77: 287-301.

[27] Arya Y, Kumar N. BFOA-scaled fractional order fuzzy PID controller applied to AGC of multi-area multi-source electric power generating systems. Swarm Evol Comput 2017; 32: 202-218.

[28] Debbarma S, Saikia LC, Sinha N. Automatic generation control using two degree of freedom fractional order PID controller. Electr Pow Energ Syst 2014; 58: 120-129.

[29] Taher SA, Fini MH, Aliabadi SF. Fractional order PID controller design for LFC in electric power systems using imperialist competitive algorithm. Ain Shams Eng J 2014; 5: 121-135.

[30] Sondhi S, Hote YV. Fractional order PID controller for load frequency control. Ener Conv Manag 2014; 85: 343-353.

[31] Sondhi S, Hote YV. Fractional order PID controller for perturbed load frequency control using Kharitonov's theorem. Electr Pow Energ Syst 2016; 78: 884-896.

[32] Shayeghi H, Shayanfar HA, Jalili A. Load frequency control strategies: a state of-the-art survey for the researcher. Ener Conv Manag 2009; 50: 344-353.

[33] Pandey SK, Mohanty SR, Kishor N. A literature survey on load–frequency control for conventional and distribution generation power systems. Renew Sust Energ Rev 2013; 25: 318-334.

[34] Tan W. Tuning of PID load frequency controller for power systems. Ener Conv Manag 2009; 50: 1465-1472.

[35] Tan W. Unified tuning of PID load frequency controller for power systems via IMC. IEEE T Pow Sys 2010; 25: 341-350.

[36] Saxena S, Hote YV. Load frequency control in power systems via internal model control scheme and model-order reduction. IEEE T Pow Sys 2013; 28: 2749-2757.

[37] Padhan DG, Majhi S. A new control scheme for PID load frequency controller of single-area and multi-area power systems. ISA T 2013; 52: 242-251.

[38] Anwar N, Pan S. A new PID load frequency controller design method in frequency domain through direct synthesis approach. Electr Pow Energ Syst 2015; 67: 560-569.

[39] Chen TC, Chang CY, Han KW. Model reduction using the stability-equation method and the continued-fraction method. Int J Cont 1980; 32: 81-94.